The Design of a High Gain Dual-Polarized Quad-Ridged Circular Horn Antenna for Wideband EMC Test Applications

Bekir Solak [1,3], Mustafa Secmen [2], and Ahmet Tekin [3]

[1] TUBITAK Space Technologies Research Institute
Microwave and Antenna Systems Group, Ankara, Turkey
bekir.solak@tubitak.gov.tr

[2] Department of Electrical and Electronics Engineering
Yasar University, Bornova, Izmir, 35100, Turkey
mustafa.secmen@yasar.edu.tr

[3] Department of Electrical and Electronics Engineering
Ozyegin University, Cekmekoy, Istanbul, 34794, Turkey
ahmet.tekin@ozyegin.edu.tr

Abstract ─ This paper presents the design of a high gain broadband quadruple-ridged circular horn antenna for Electromagnetic Compatibility (EMC) testing. The proposed antenna contains a wideband feed structure as a transition between coaxial line and quad-ridged circular waveguide behind the conical horn antenna. The wideband matching between impedances at the apertures of the feed and the horn is achieved with a tapering at the flare section along the horn length, which is obtained after a detailed investigation of various tapering profiles. The antenna is designed to operate in horizontal and vertical polarizations (dual linear polarization) simultaneously in EMC tests. This implementation is found to present a return loss greater than 10 dB, isolation level higher than 28 dB, high-gain (minimum 13.6 dBi) and low-gain variation of 4.5 dBi within the frequency range of 1-6.75 GHz (6.75:1 bandwidth) at both polarizations, which is a desired feature in radiated emission and immunity tests.

Index Terms ─ Circular horn antenna, dual polarization, Electromagnetic Compatibility (EMC), quad-ridged circular waveguide, wideband antenna.

I. INTRODUCTION

Electromagnetic Compatibility (EMC) can simply be explained as how well a device or system is able to operate in an electromagnetic environment without introducing electromagnetic disturbances, which can interfere with the operation of the other electrical products. The EMC standards contain the requirements for the qualification of a particular electronic product that depends on application area in which the product is to be used. EMC studies the unintentional generation, propagation, and reception of electromagnetic energy [1]. EMC issues can be investigated in two main categories. Radiated emission is related to the unwanted generation of the electromagnetic signal from the product which can spoil the proper operation of the other products. Immunity or susceptibility on the other hand can be considered to be reverse process of the radiated emission where the proper operation of the equipment under test (EUT) exposed to an electromagnetic field is investigated [2]. Tests of both radiated emission and immunity are carried out for a wide frequency bandwidth such as 1-6 GHz with respect to the EMC standards [3]; and hence, wideband antennas should be used for this purpose.

Horn antennas are commonly used for many applications such as radar, radio astronomy, electronic warfare and tests/measurements such as EMC tests. Broadband horn antennas have received more attention in EMC test applications in comparison to other wideband antenna candidates such as biconical and log-period antennas since the horn antennas can provide higher gain, better return loss and more compact structures [4]. Besides, as an important issue in the EMC measurement to save a significant amount of time in the tests, the horn antennas can be used in dual linear polarization simultaneously, which is not easily possible with a single biconical and log-periodic antennas of broadband applications. The traditional horn antennas (pyramidal or conical); however, are originally narrow band where the feed standard rectangular or circular waveguides behind them limits the operation frequency bandwidth [5,6].

The usage of ridges in the rectangular or circular waveguide was shown to give a single mode operation for a substantially wider bandwidth by decreasing the

Submitted On: June 4, 2017
Accepted On: October 8, 2018

cutoff frequency of the dominant mode [7-10]. The ridge waveguides, which also become the solution of limited bandwidth problem of the horn antennas, are frequently used for the excitation of wideband horn antennas. In order to give proper matching in the broadband, the ridges should be also used in the flare section of the horn antennas.

The double ridge horn antennas with the double ridged waveguides behind can give single linear polarization [11]. It is shown with the relevant studies that extremely wideband operation can be satisfied for the frequency band of 2-18 GHz (9:1 bandwidth) [12], 1-18 GHz (18:1 bandwidth) [13,14] and even for 2-40 GHz (20:1 bandwidth) [15] by providing VSWR≤2 or $S_{11} \leq$ -9.5 dB (return loss ≥ 9.5 dB). The bands of these single linear polarized antennas are sufficiently enough for EMC tests covering radiation emission and immunity measurements with the frequency bandwidth of 6:1.

In radiated emission and immunity tests, the measurements are generally acquired for both two orthogonal linear polarizations (vertical and horizontal). For this purpose, the EMC tests done with single linear polarized (double-ridged) antennas should be realigned for each polarization case (single vertical and single horizontal), which increases the measurement time significantly. Therefore, recently, dual linear polarized antennas, which are able to take the measurements of both polarizations at once, are becoming more popular. The dual polarization in the horn antennas can be realized by using quadruple ridges both in the waveguide behind horn and in the flare of the horn along axial direction. However, the usage of quad-ridged structure reduces the bandwidth significantly due to excitation of additional higher-order modes as compared to double-ridged case such that the ultra-wideband operations such as 9:1, 18:1 or 20:1 bandwidth cannot be obtained easily. For broadband applications, the square and circular cross-sections are used. However, when the studies with square horn in [16] and circular horn in [17], which give VSWR ≤ 2.6 and VSWR ≤ 2.2 for 8-18 GHz, respectively; and the square and circular structures giving 4:1 and 6:1 bandwidth, respectively in [18] are investigated, the circular (conical) horn antennas can be stated to give better performance. This has led to the choice of circular cross-section in the proposed study.

The antennas used in EMC radiated emission and immunity test are desired to have high gain and low gain variation (almost constant gain) as well as low VSWR and dual linear polarization characteristics. When most of the reported studies with circular or square quad-ridged horn antennas for wideband applications were investigated [17,19-21], it was noticed that none could provide return loss higher than 10 dB (or VSWR≤1.925) for 6:1 frequency bandwidth, which is very much needed for radiated emission and immunity tests at 1-6 GHz. Two recent designs [22, 23] among these studies have improved results by giving return losses higher than 10 dB at both ports, i.e. $S_{11} \leq$ -10 dB and $S_{22} \leq$ -10 dB, within almost 6:1 bandwidth (1.66-10 GHz in [22] and 2-12 GHz) in [23]). However, the performances of minimum gain and gain variation within the frequency band are not so satisfactory such that the work in [22] approximately reports minimum 8 dBi gain at the lower part of the frequency band, and a gain variation of 10 dB within the band; while the design in [23] has about 10 dBi minimum gain, and 8 dB variation.

In this paper, a circular horn antenna with quadruple ridges in the flare of the horn and in the circular waveguide behind the antenna is designed. The proposed antenna works at the EMI test frequency band of 1-6.75 GHz (6.75:1 bandwidth) by yielding a reflection coefficient below -10 dB (VSWR≤1.925), minimum 13.6 dBi gain and about 4.5 dB gain variation within the band with dual polarization feature. This special antenna, which is designed to cover the frequency bands of EMC radiated emission and immunity tests, has also minimum isolation of 28 dB between ports. The antenna achieves the mentioned performance metrics with a quad-ridged circular waveguide including a specially designed back cavity to make a proper transition from coaxial feed to the quadruple circular waveguide, and a conical horn with a x^p tapered ridge profile, which is obtained as a result of a detailed profile and parametric investigations.

The rest of the paper is organized as follows: Section II includes the design and results for the transition from coaxial to quad-ridged circular waveguide, which consists of a special back cavity to suppress the effects of undesired higher order modes inside the circular waveguide. As to the design part of circular horn, the investigation of possible ridge profiles inside the conical horn and the parameter study of the ratio of aperture radius to circular waveguide radius (the radius of the beginning of the flare) are given in Section III. Finally, CST Microwave Studio simulation results of the overall antenna are presented in Section IV, followed by the conclusion in Section V.

II. THE DESIGN OF COAXIAL TO QUAD-RIDGED CIRCULAR WAVEGUIDE AS THE FEED OF CIRCULAR HORN ANTENNA

As stated in Section I, the ridged waveguides can supply wider bandwidth in comparison to hollow waveguides by decreasing the cutoff frequency of the dominant mode and increasing the frequency bandwidth between the dominant mode and the second lowest mode (second higher order mode). However, as described in [8] and [10], in the case of quadruple ridged waveguide, although the insertion of ridges decreases the cutoff frequency of the fundamental mode would also reduce the cutoff frequency second lowest mode. The cutoff frequency of second lowest mode becomes very close to that of the fundamental mode when the ridge is heavily

loaded, i.e., the gap between the ridges are so small. Therefore, if a single mode operation is desired, the effect of the second lowest mode should be suppressed. In the circular quad-ridge waveguide case, the dominant mode is TE_{11} mode and the second lowest one is TE_{21L}, which arises from the splitting of TE_{21} mode into TE_{21L} and TE_{21U}. Besides, if a wideband operation with about 6:1 bandwidth is desired, other higher modes such as TE_{21U}, TE_{01}, TE_{31} and TM_{01} modes of circular quad-ridged waveguide should be also taken into account that the cutoff frequencies of these modes probably fall into the frequency region of interest. Therefore, the transition from coaxial to quad-ridged waveguide should be carefully designed to annihilate the effects of these higher order modes. The design of the mentioned transition is critical in terms of return loss and isolation performances of the overall antenna structure. The circular horn part of the overall antenna design does not significantly deteriorate the reflection and isolation performance of the overall antenna structure when a smooth tapering is used for the ridges inside the flared circular horn. Therefore, the return loss and isolation performances are mainly determined with the feed waveguide part of the overall design.

The suppression of these higher order modes and especially for the most crucial higher order mode of TE_{21L} cannot be achieved successfully by just arranging the probe of SMA connector inserted into the standard circular quad-ridged waveguide whose one side is back shorted with a metallic plate along the propagation axis without the addition of any cavity. This is because the suppression of TE_{21L} mode also makes a reduction in the effect of TE_{11} mode since the cutoff frequencies of both modes are close to each other. Therefore, in order to provide a wider bandwidth, a back cavity structure behind the feeding pins is generally used.

In [17] and [18], the cylindrical and conical back cavities are implemented; however, the overall most of these structures were reported to yield no more than 3:1 bandwidth which is not sufficient for EMC emission and immunity tests. In this study, a transition depicted in Fig. 1 is designed to acquire satisfactory reflection and isolation performance. When the structure in Fig. 1 is investigated, there is a back-shorted part behind feed probes, which has the cross section of a quadruple circular waveguide with different ridge dimensions than feed quadruple circular waveguide. Therefore, hollow circular waveguide cavity used in [17] is replaced with a quadruple circular waveguide.

In the design of this study, it is targeted to obtain reflection coefficient lower than -10 dB for both ports ($S_{11} \leq$ -10 dB and $S_{22} \leq$ -10 dB), isolation greater than 30 dB, and the transmission coefficients of all possible and effective higher order modes such as TE_{21U}, TE_{01}, TE_{31} and TM_{01} modes lower than -10 dB for an effective suppression of these undesired modes. The dimensions of the designed transition structure are obtained after performing an optimization process in CST Microwave Studio. The corresponding dimensions are given in Fig. 2 along with relevant cut views of the structure where the optimum radius of circular waveguide is found to be about r_i = 57.12 mm. For the given radius of circular waveguide, the corresponding cutoff frequencies of TE_{11}, TM_{01}, TE_{21}, TE_{01} and TE_{31} modes can be calculated approximately as 1.54 GHz, 2.01 GHz, 2.56 GHz, 3.21 GHz and 3.52 GHz, respectively, for a standard hollow circular waveguide [24]. Therefore, this standard hollow circular waveguide without any ridges inside can only operate within 1.5-2 GHz for a single mode operation, and even TM_{01} mode is suppressed, its bandwidth is not more than 1.66:1. If a frequency band of 1-6.75 GHz is desired, the cutoff frequency of fundamental TE_{11} mode should be decreased to below 1 GHz.

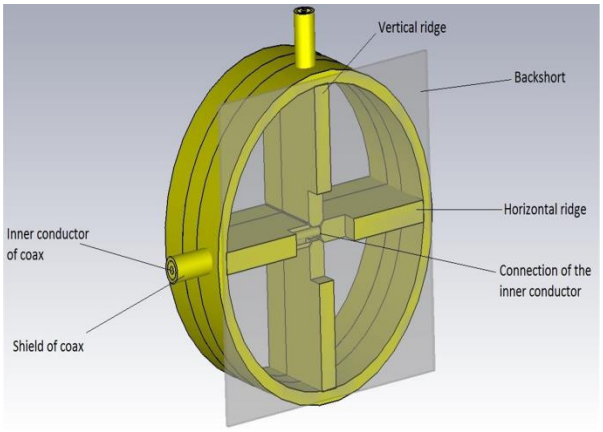

Fig. 1. The designed structure for the transition from coaxial feeds to circular quad-ridged waveguide where back-short metallic wall is deliberately shown as transparent.

When the quad-ridged dimensions given in Fig. 2 is used following the optimization process, it is verified in CST Microwave Studio that the cutoff frequencies of TE_{11}, TE_{21L}, TE_{21U}, TE_{01}, TE_{31} and TM_{01} are 0.346 GHz, 0.352 GHz, 2.767 GHz, 3.472 GHz, 3.634 GHz and 4.766 GHz. So, the cutoff frequency of TE_{11} mode is pushed below 1 GHz, and that of TM_{01} mode increases significantly as expected. However, again as expected, the cutoff frequency of the second lowest mode of TE_{21L} becomes quite close to TE_{11} mode. Since the desired frequency band is between 1 GHz and 6.75 GHz, the higher modes of TE_{21L}, TE_{21U}, TE_{01}, TE_{31} and TM_{01} whose cutoff frequencies are below 6.75 GHz should be suppressed as much as possible. This suppression is achieved by using a modified back cavity whose dimensions are given in Fig. 2 (b).

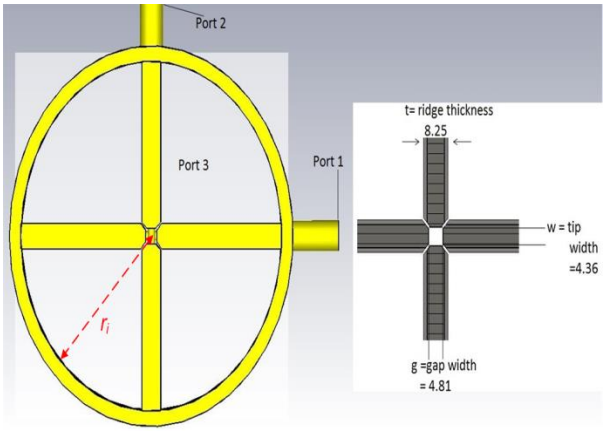

(a)

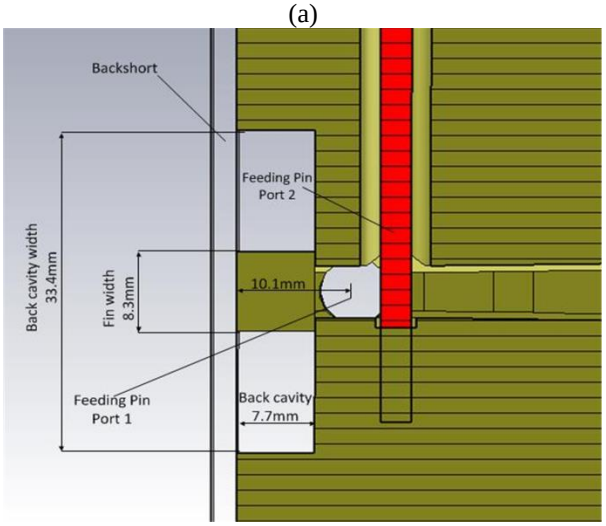

(b)

Fig. 2. (a) The front view of the designed transition structure and the relevant dimensions in mm, and (b) the side view of the designed transition structure and the relevant dimensions in mm.

The results corresponding to suppression of these modes are shown in Fig 3 (a) and 3(b) for the excitation from port 1 and port 2, respectively where the values below -40 dB are not presented for a better view. The reflection coefficients (S_{11} and S_{22}) and isolation between ports (S_{12} and S_{21}) are also given in addition to transmission coefficients (S_{31} for port 1 and S_{32} for port 2) of undesired modes. As it can be observed from the results in Fig. 3, all of the undesired higher order modes taken into account are suppressed more than 10 dB within the frequency band of 1-6.75 GHz for each port such that most of these modes are reduced by 15 dB within the given frequency band. Besides, the isolation is found to be more than 30 dB throughout the given band as desired. Finally, the reflection is below -10 dB for 1-6.75 GHz for the excitation of port 1, and 1-6.5 GHz for the excitation of port 2.

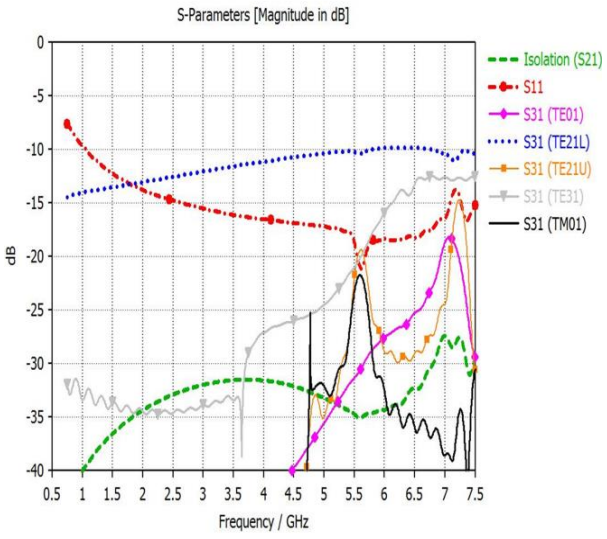

(a)

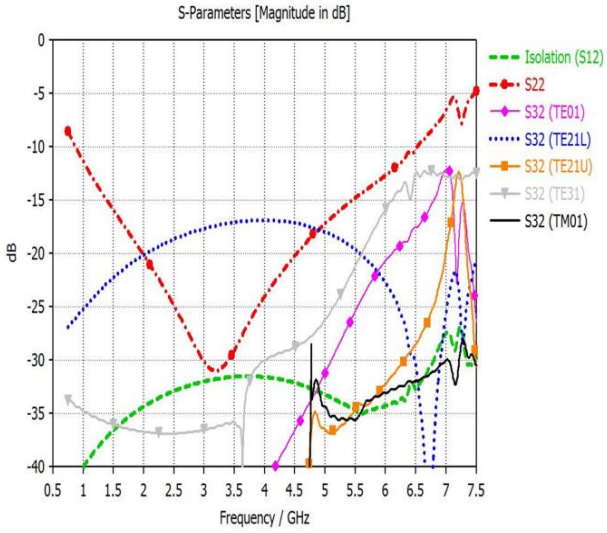

(b)

Fig. 3. (a) The reflection coefficient (S_{11}), isolation and transmission values (S_{31}) of undesired modes for port 1, and (b) the reflection coefficient (S_{22}), isolation and transmission values (S_{32}) of undesired modes for port 2.

III. QUAD-RIDGED CIRCULAR HORN ANTENNA STRUCTURE

After the determination of the transition from SMA feed connectors to quad-ridged circular waveguide, the design details of a circular horn section having quadruple ridges at the flare extension are presented. The quad-ridge circular waveguide structure of the previous section is arranged to match the mentioned flare extensions of the horn part. Due to the strict requirements of the application itself, the final antenna structure is expected to maintain about 13 dBi gain for 1-6.75 GHz

full-band in order to attain high gain characteristics for the antenna. In the aperture antennas including horn antennas, the minimum gain is usually achieved at the lowest frequency. Therefore, it is aimed to get minimum 13.75 dBi gain at 1 GHz for the design in consideration. The approximate and classical gain formula for circular horn antenna is given as [5]:

$$G(dBi) = 10log_{10}\left[\varepsilon_{ap}\frac{4\pi}{\lambda^2}\left(\pi a_{horn}{}^2\right)\right], \quad (1)$$

where ε_{ap} is the aperture efficiency, λ is the wavelength and a_{horn} is the radius at horn aperture. By taking maximum wavelength as $\lambda = 30$ cm (wavelength at f = 1 GHz) and ε_{ap} about 0.51 according to [5], the aperture radius of horn is approximately calculated to be a_{horn} = 32.7 cm for the desired minimum gain of 13 dBi. Then, the axial length (AL) of the horn is evaluated by using the curves given in [25], which relates the gain, diameter of the circular horn and axial length. The axial length of the designed horn is calculated as approximately AL = 2.1λ, which corresponds to about AL = 63 cm. The patterns of the ridges and sidewall of double or quadruple ridged circular horn antennas are usually determined with some special profile functions for a smooth taper between feed waveguide and horn aperture. All profiles, which are described as a radius value any z point at axial direction in [26], contain the parameters of L (length along axial direction), a_i (the radius at the feed point when z = 0) and a_o (the radius at the aperture point when z = L). For instance, the profile selected in this study, which is x^p profile, has the function of:

$$a(z) = a_i + (a_o - a_i)\left[(1-A) + A\left(\frac{z}{L}\right)^p\right], \quad (2)$$

where p is exponent parameter, and A is the linearity parameter. The ridge shape inside the circular horn can be categorized as un-truncated and truncated where a sample view of truncated ridge shape is depicted in Fig. 4. This particular design choice was preferred in this study. In the un-truncated ridge shape, the length parameter in (2) is selected as axial length (AL); consequently, taper length becomes equal to AL in Fig. 4. Besides, the radii at the aperture point parameter a_o are selected a_{horn} for both ridge and sidewall tapers, which gives $a_{horn} = a_{side} = a_{ridge}$. Consequently, the curves for ridge and sidewall tapers approach to a point at z = AL to form a tip at the end side of the ridge. In other words, the part without ridge in Fig. 4 is filled by a ridge structure giving a ridge shape with one side is a tip point and another side an edge.

In the truncated ridge shape, the length parameter in (2) is selected as taper length (TL) in Fig. 4, which was smaller than AL. Besides, $a_{horn} > a_{side} > a_{ridge}$ should be satisfied as given in Fig. 4. By satisfying these conditions, a ridge shape having edges at the both sides as shown in Fig. 4 was attained. The truncated ridge structure has more flexibility and more design parameters with additional degrees of freedom in comparison to un-truncated one. Actually, when the studies in [17] and [18] utilizing from un-truncated ridges and the one in [23] using truncated ridges are compared, the superiority of the truncated ridges can be observed since it clearly yields a wider bandwidth. Therefore, the truncated ridge profiles rather were considered in the design. A thorough examination is carried out for several different profile functions (exponential, polynomial, x^p, etc.), taper length values (L value in profile functions) and radii at the ridge and sidewall aperture points (a_o values in profile functions). During this optimization process with advanced EM tools, the radii at the feed waveguide point (a_i values in profile functions) were kept as $a_{i,ridge}$ = 2.4 mm and $a_{i,sidewall}$ = 57.12 mm, which corresponds to half of the gap width in Fig. 2 (b) and radius of the feed quadruple circular waveguide, respectively. Besides, the axial length was fixated at AL = 63 cm. The conditions of L = TL < AL and $a_{horn} > a_{side} > a_{ridge}$ were found to be appropriate design parameters. The same profile functions were applied for both ridge and sidewall tapering during the design work. The optimization was strictly aimed to yield the minimum 13 dBi flat gain within 1-6.75 GHz with minimal fluctuations. As a result of the profile study, the x^p tapering is found to give best results with the parameters of p = 2.15, A = 1, TL = 56.4 cm and $a_{o,ridge}$ = 26.2 mm for ridge taper and p = 2.4, A = 1, TL = 60.3 cm and $a_{o,ridge}$ = 28.15 mm for sidewall taper in (2).

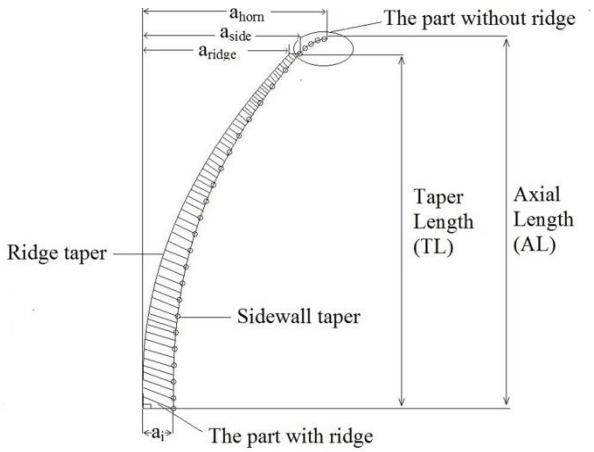

Fig. 4. The geometry of a truncated ridge in a circular horn antenna used in this study.

Among several simulations that were carried out, one crucial result is the comparison of possible profile functions. The corresponding results are depicted in Fig. 5 at which the gain values of the antennas' designs with different profiles for port 1 are given (where the results for port 2 are also similar). From the results in Fig. 5, the

x^p function has the gain between 13.7 dBi and 18.1 dBi in the frequency band of 1-6.75 GHz. The resultant gain variation is only about 4.4 dBi, which is lowest among all possible profiles.

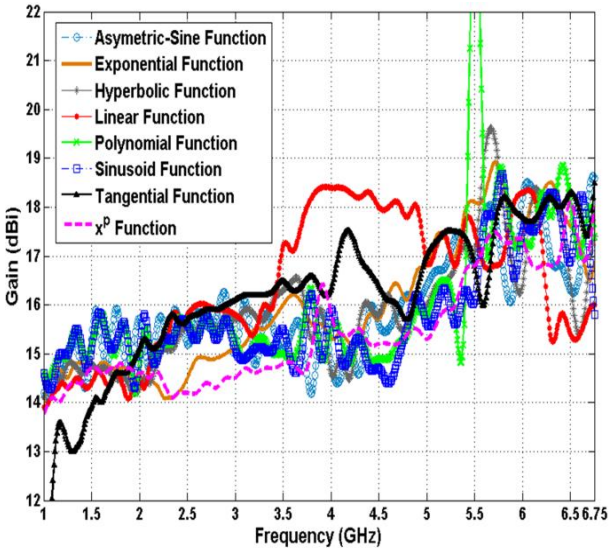

Fig. 5. The gain of the designed antenna for different profile functions when port 1 is excited.

After the reveal of the necessary parameters for the design of the ridges and circular horn antenna, an additional parameter about the feed waveguide dimension was explored. The aim of this analysis was to observe whether a modification in the feed waveguide structure improved the performance of the overall antenna or not. For this purpose, since $a_{i,sidewall}$ = 57.12 mm is also equal to radius of feed quad-ridged circular waveguide behind the antenna, the value of $a_{i,sidewall}$ is varied by keeping all the parameters in the horn antenna part constant including $a_{o,sidewall}$ = 28.15 cm. Since the radius of the circular waveguide has changed, all the dimensions of the transition including back cavity described in Section II were rearranged accordingly. The ratio of a_o/a_i is equal to 281.5 mm/57.12 mm = 4.93 for the sidewall tapering of the original antenna, and this ratio is varied (increased and decreased) by keeping a_o value constant as 28.15 cm. The corresponding results for different a_o/a_i values are demonstrated in Fig. 6. According to results in Fig. 6, the original antenna with a_o/a_i = 4.93 still has minimum gain variation with 13.7 dBi minimum gain within the frequency band as compared to other ratio values. The ratio of a_o/a_i = 5.22 possesses very close results to those of a_o/a_i = 4.93; however, the original antenna gives slightly better results. Thus, this analysis also validates the transition structure.

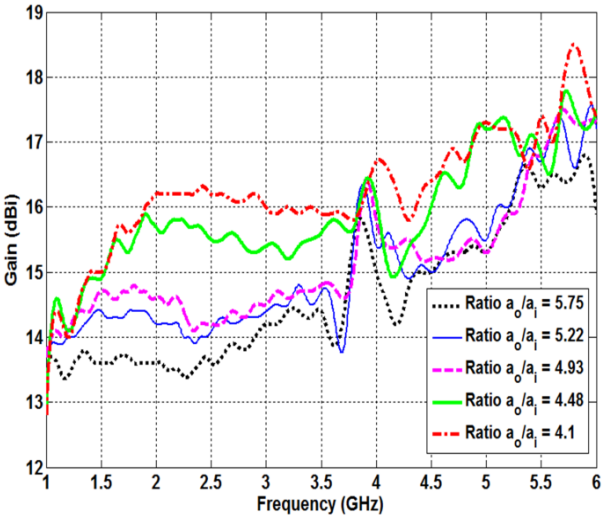

Fig. 6. The gain of the designed antenna for different a_o/a_i ratio values when port 1 is excited.

IV. THE RESULTS OF THE OVERALL ANTENNA

After the reveal of the necessary parameters for the design of the ridges and circular horn antenna with x^p profile ridges are completed, the final minor modifications on the overall antenna structure were done to acquire the concluding results of the antenna. The first slight modification realized on the resulting antenna is the addition of traditional curved-surface sections to the outside of the aperture edges of the circular horn antenna [5]. This insertion generally reduces the undesired diffraction from the edge of the aperture of the horn, which prevents the spoil of this diffraction on the radiation pattern. It also results in a slight improvement on the return loss performance of the antenna. The second modification is the realization of all final simulations with aluminum material for all parts of the designed antenna. The simulations realized in Section III are carried out with perfect electric conductor (PEC) in order to obtain the results more quickly. However, after the final design of the overall antenna was ensured, the simulations were repeated with aluminum to be more suitable for the practical low cost implementation. The simulation view of the final antenna design is depicted in Fig. 7, and the results are collected by exciting each horizontal and vertical polarization port one by one.

First, the reflection coefficient (return loss) and isolation performances of the final structure are examined. The results are shown in Fig. 8 such that the reflection coefficients are below -10 dB (VSWR $\leq$ 1.925) for the desired frequency band of 1-6.75 GHz. The connection of the designed circular horn antenna to the output of

the transition described in Section II and the final modifications on the antenna do also improve overall return loss performance of the transition. When the reflection coefficient results of the transition for port 2 given in Fig. 3 (b) is examined, the values are higher than -10 dB especially for the problematic frequency region of 6.5-6.75 GHz. However, the values came out below -10 dB in the final antenna design as shown in Fig. 8 for this troubling region of port 2. The isolation performance of the overall antenna is found to better than 28 dB for the whole frequency band. In comparison to the isolation results of the transition, which is higher than 30 dB, the antenna shows a small drop of about 2 dB in the isolation performance value; however, the isolation value of minimum 28 dB over the total frequency band can be still considered as sufficient for the target EMC application.

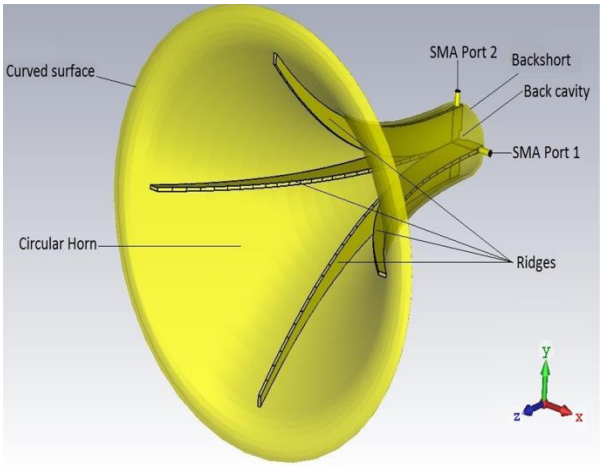

Fig. 7. The simulation view of the designed quad-ridged circular horn antenna.

The next performance parameter investigated was the gain values of the designed antenna at each polarization and gain variation within the frequency band of 1-6.75 GHz. The corresponding simulation results are shown in Fig. 9.

According to the gain results in Fig. 9, the minimum gain is found to be 13.6 dBi for both polarizations and almost 4.5 dBi (between 13.6 dBi and 18.1 dBi) gain variation was observed. This gain variation is lower than the other similar studies in the literature hence the antenna in this work can be regarded to have almost constant gain as well.

As the final analysis in this section, the radiation patterns of the proposed antenna are investigated. The radiation patterns are given for only port 1 in Fig. 10 at some sample frequencies (at the center and edge frequencies). According to these patterns in Fig. 10, the antenna is directed towards to broadside direction without any significant shift in the beam for both E- and H-planes. Moreover, the cross-polar levels are found to be low such that the lowest co-polar to cross-polar ratio (XPD) within 3 dB beamwidth of co-polar patterns is found to be 22.5 dB and 13 dB for E- and H-planes, respectively at the frequency band of 1-6.75 GHz.

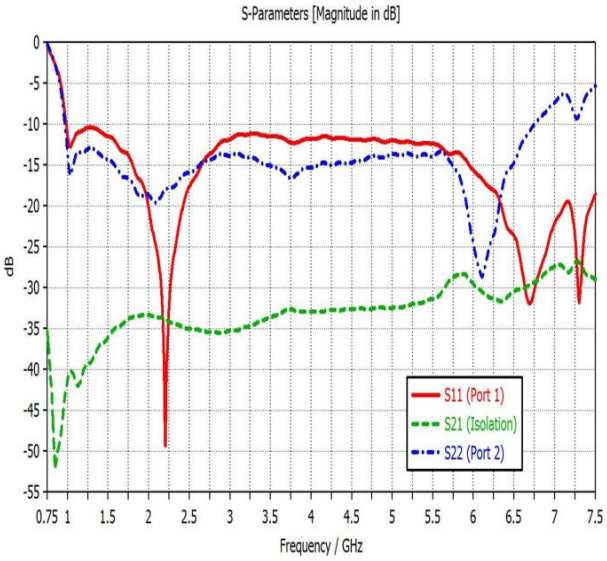

Fig. 8. The reflection coefficients of each port and isolation between ports of the proposed antenna.

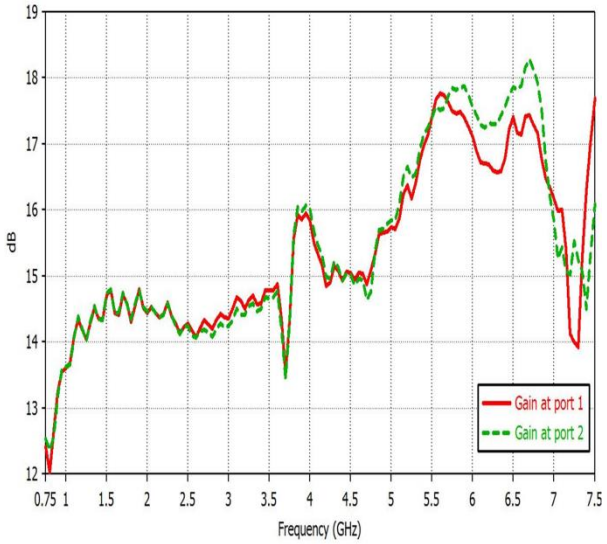

Fig. 9. The gain versus frequency of the proposed antenna for each port (linear polarization).

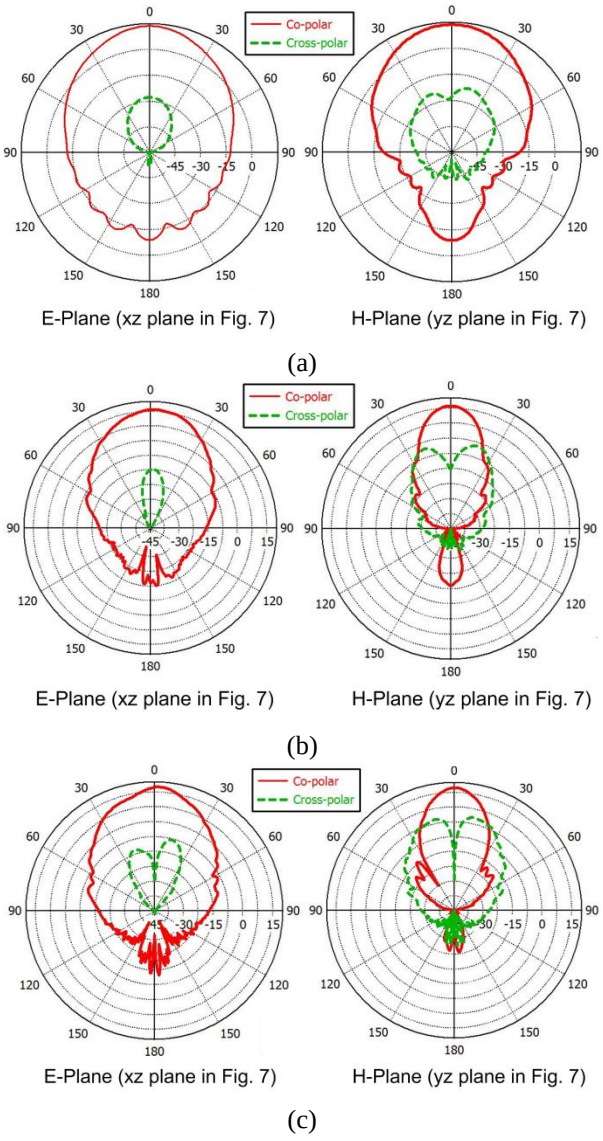

Fig. 10. The E-plane and H-plane radiation patterns of the proposed antenna for port 1 at: (a) 1 GHz, (b) 4 GHz, and (c) 6.75 GHz.

V. CONCLUSION

In this paper, the quad-ridged horn antenna is designed based on detailed profile examinations and the parametric studies. A dual-polarized quad-ridged horn is presented that achieves 6.75:1 frequency bandwidth for the both polarization cases. Moreover, the simulation results of the designed antenna has shown low return loss (>10 dB), low VSWR (<1.925), high isolation (>28 dB), high gain (minimum 13.6 dBi) and reasonable radiation patterns with low cross-polarization level over the operation frequency range 1-6.75 GHz. The antenna is designed to operate in the horizontal and vertical polarizations (dual linear polarization) simultaneously for EMC testing applications (radiated emission and radiated immunity tests). Compared with the conventional circular quad-ridge horn antennas and other similar studies, the designed antenna achieves better gain at lower frequencies, almost constant gain (a variation of 4.5 dBi) and wider frequency bandwidth.

REFERENCES

[1] D. G. Baker, *Electromagnetic Compatibility: Analysis and Case Studies in Transportation*. John Wiley & Sons Inc., Hoboken, NJ, USA, 2016.

[2] T. Williams, *EMC for Product Designers: Meeting the European EMC Directive*. Newnes, Oxford, UK, 2014.

[3] ETSI EN 301 489-17, Electromagnetic Compatibility and Radio Spectrum Matters (ERM); Electro-Magnetic Compatibility (EMC) Standard for Radio Equipment; Part 17: Specific Conditions for Broad-band Data Transmission Systems, 2016.

[4] M. Abbas-Azimi, F. Arazm, J. R. Mohassel, and R. Faraji-Dana, "Design and optimization of a new 1-18 GHz double ridged horn antenna," *Journal of Electromagnetic Wave Appl.*, vol. 21, no. 4, pp. 501-506, Apr. 2007.

[5] C. A. Balanis, *Antenna Theory: Analysis and Design*. 3rd ed., John Wiley & Sons Inc., Hoboken, NJ, USA, 2005.

[6] T. A. Milligan, *Modern Antenna Design*. 2nd ed., John Wiley & Sons Inc., Hoboken, NJ, USA, 2005.

[7] S. B. Cohn, "Properties of ridged waveguide," *Proc. IRE*, vol. 35, no. 8, pp. 783-788, Aug. 1947.

[8] M. H. Chen, G. N. Tsandoulas, and F. G. Willwerth, "Modal characteristics of quadruple-ridged circular and square waveguides," *IEEE Trans. Microwave Theory and Tech.*, vol. 22, no. 8, pp. 801-804, Aug. 1974.

[9] W. Sun and C. A. Balanis, "MFIE analysis and design of ridged waveguides," *IEEE Trans. Microwave Theory and Tech.*, vol. 41, no. 11, pp. 1965-1971, Nov. 1993.

[10] W. Sun and C. A. Balanis, "Analysis and design of quadruple-ridged waveguides," *IEEE Trans. Microwave Theory and Tech.*, vol. 42, no. 12, pp. 2201-2207, Dec. 1994.

[11] A. Mallahzadeh and H. Ahmadabadi, "Design of N-channel rotary joint using curved double-ridged waveguide and concentric coaxial lines," *Applied Computational Electromagnetics Society (ACES) Journal*, vol. 27, no. 1, pp. 50-58, Jan. 2012.

[12] A. Mallahzadeh and A. Imani, "Modified double ridged antenna for 2-18 GHz," *Applied Computational Electromagnetics Society (ACES) Journal*, vol. 25, no. 2, pp. 137-143, Feb. 2010.

[13] C. Burns, P. Leuchtmann, and R. Vahldieck, "Analysis and simulation of a 1-18 GHz broadband double-ridged horn antenna," *IEEE Trans. Electromagn. Compat.*, vol. 45, no. 1, pp. 55-60, Feb.

2003.
[14] M. Abbas-Azimi, F. Arazm, and R. Faraji-Dana, "Design and optimisation of a high-frequency EMC wideband horn antenna," *IET Microw. Antennas and Propag.*, vol. 1, no. 3, pp. 580-585, June 2007.
[15] N. Z. Tenigeer, Q. Jinghui, Z. Pengyu, and Z. Yang, "Design of a novel broadband EMC double ridged guide horn antenna," *Progress in Elec. Res. C*, vol. 39, pp. 225-236, 2013.
[16] R. Dehdasht-Heydari, H. R. Hassani, and A. R. Mallahzadeh, "Quad ridged horn antenna for UWB applications," *Progress in Elec. Res.*, vol. 79, pp. 23-38, 2008.
[17] A. R. Mallahzadeh, A. A. Dastanj, and S. Akhlaghi, "Quad-ridged conical horn antenna for wideband applications," *International Journal of RF Microwave CAE.*, vol. 19, no. 5, pp. 519-528, Sept. 2009.
[18] A. Akgiray and S. Weinreb, "Ultrawideband square and circular quad-ridge horns with near-constant beamwidth," *IEEE ICUWB Ultrawideband Conference*, Syracuse, NY, USA, pp. 518-522, Sept. 2012.
[19] Z. Shen and C. Feng, "A new dual-polarized broadband horn antenna," *IEEE Antennas and Wireless Propagation Letters*, vol. 4, no. 1, pp. 270-273, 2005.
[20] R. Dehdasht-Heydari, H. R. Hassani, and A. R. Mallahzadeh, "A new 2-18 GHz quad-ridged horn antenna," *Progress in Elec. Res.*, vol. 81, pp. 183-195, 2008.
[21] J. Liu, Y. Zhou, and J. Zhu, "Research and design of quadruple-ridged horn antenna," *Progress in Elec. Res. Lett.*, vol. 37, pp. 21-28, 2013.
[22] P. H. Van der Merwe, J. W. Odendaal, and J. Joubert, "An optimized quad-ridged horn antenna with pyramidal sidewalls," *Journal of Elec. Waves and Appl.*, vol. 27, no. 17, pp. 2263-2273, Sept. 2013.
[23] A. Akgiray, S. Weinreb, W. A. Imbriale, and C. Beaudoin, "Circular quadruple-ridged flared horn achieving near-constant beamwidth over multi-octave bandwidth: Design and measurements," *IEEE Trans. Antennas Propagat.*, vol. 61, no. 3, pp. 1099-1108, Mar. 2013.
[24] D. M. Pozar, *Microwave Engineering*. 4rd ed., John Wiley & Sons Inc., Hoboken, NJ, USA, 2012.
[25] A. P. King, "The radiation characteristics of conical horn antennas," *Proc. IRE*, vol. 38, no. 3, pp. 249-251, Mar. 1950.
[26] C. Granet, "Profile options for feed horn design," *Asia-Pacific Microwave Conference*, Sydney, Australia, pp. 518-522, Dec. 2000.

Bekir Solak was born in Denizli, Turkey in 1988. He received the B.S. degree from Department of Electronics and Communication Engineering, Izmir Institute of Technology, Izmir, Turkey in 2012. Then, he has received his M.Sc. from Department of Electrical and Electronics Engineering, Ozyegin University, Istanbul in 2017. He has been an EMC Engineer in Tubitak Space Technologies Research Institute, Ankara since 2018. His current research interests are the analysis and design of horn antennas for EMC applications.

Mustafa Secmen was born in Izmir, Turkey in 1980. He received the B.S. and Ph.D. degrees from the Department of Electrical and Electronics Engineering, Middle East Technical University, Ankara, Turkey, in 2002 and 2008, respectively. He has been a Professor with Department of Electrical and Electronics Engineering, Yasar University, Izmir since 2010. His current research interests include radar signal processing, microwave component and antenna design for satellite/mobile communications, horn and smart antennas.

Ahmet Tekin has received his EE Ph.D. degree from University of California Santa Cruz, CA, EE MS degree from North Carolina A&T State University, Greensboro, NC and EE BS degree from Bogazici University, Istanbul, Turkey in 2008, 2004, and 2002, respectively. In addition to academic research, he worked for many innovative semiconductor design companies such as; Multigig, Inc., Newport Media, Aydeekay LLC, Broadcom corp., Semtech Corp., Nuvoton Technology Corp., Qualcomm and Waveworks Inc., leading microelectronic designs for communications, consumer and medical markets. His main focus area is analog/RF/mixed-signal integrated circuit design for communication and biomedical applications. He is currently a Faculty Member at Ozyegin University Electrical and Electronics Engineering Department and a Cofounder at Waveworks Inc.